

UCRL--15648

DE85 006255

COMPARATIVE SINTERABILITY OF COMBUSTION
SYNTHESIZED AND COMMERCIAL TITANIUM CARBIDES

Barry Wayne Manley
University of California, Davis
Davis, CA

November 1984

Lawrence
Livermore
National
Laboratory

CONTENTS

I.	Introduction	p. 1
II.	Materials and Methods	p. 16
III.	Results	p. 27
IV.	Discussion	p. 34
V.	Summary	p. 47
VI.	Acknowledgments	p. 49a
VII.	References	p. 50

I. Introduction

The means by which powdered refractory compounds are produced can influence their mechanical and structural properties.¹⁻⁵ It is relevant to scrutinize these methods of powder production and examine their effects on the resulting material. One such production process is called self-propagating high-temperature synthesis (SHS), also referred to as combustion synthesis. This method has been used to produce powders which are claimed to exist in a highly stressed non-equilibrium state.¹⁻³ Such a stressed state would theoretically⁵ increase the rate of (i.e., activate) the sintering of these powders. In addition to activated sintering such properties as abrasive wear and hardness are also affected.² In the present study experiments were performed to compare the sintering kinetics of titanium carbide (TiC) produced by the SHS process, with those of titanium carbide obtained from a commercial source, the Starck Chemical Company of Germany. Possible causes for observed differences between the materials were also explored.

Merzhanov and Borovinskaya³ have described the SHS process for a variety of carbides, nitrides, and borides of the transition metals. They pressed solid reactants into pellet form and ignited them at the pellet top under an atmosphere of argon. The combustion front proceeded to propagate downwards with a zone of intense reaction activity. The rates of propagation of the reaction front varied from 0.1 to 15 cm s^{-1} . In the wake of the propagating combustion wave, luminescence continued beyond the

thermal relaxation time indicating the continuance of combustion.

According to Merzhanov and Borovinskaya³ the completeness of combustion can almost always be guaranteed by appropriate manipulation of the following reaction parameters: dispersion of reagents; bulk density of mixed reactants; size of combusting sample; heat removal from sample surface; and temperature of combustion. To this list should be added: adsorbed gases,^{6,7} impurities,⁶ stoichiometry of reactants,¹ and combusting atmosphere.⁴

In regards to some of the above parameters, Shkiro, Borovinskaya, and Merzhanov⁸ have examined the effects of various types of carbon on the combustion synthesis of titanium carbide (TiC). They found that the rate and completeness of combustion varies for different carbon powders used. The carbon powder characteristics examined were the degree of structural development, surface area, and oxygen content. Structural development is a term used in the literature⁹ to describe size of carbon chains connected by σ -sp² bonds, and the degree to which these chains are bonded to each other with the weaker π -bonds. Shkiro, Borovinskaya, and Merzhanov⁸ classified the structural development according to the carbon powders' ability to adsorb oil (oil adsorption increases with increasing structural development).

The combustion rate was found to be most sensitive to the structural development. Increasing structural development

decreased the rate and completeness of combustion. This phenomenon was associated with the decrease in free valences with an increase in structural development.

Further evidence for the influence of development on the reactivity of carbon was supplied by experiments on the effects of annealing the carbon powder before combustion. A particular grade of carbon black was annealed under vacuum at a temperature of 2373 K for time periods of 1 and 4 hours. The heat treatment relieved stresses and increased the structural development. When the resulting powders were combusted, the rate and completeness of combustion decreased with increasing annealing time. Table 1 shows the specifics of the effects of heat treatment on combustion.

The particle size of carbon black powders did not influence the combustion process in titanium carbide (TiC).⁸ However, with carbon powders with the graphite structure, a marked dependence on particle size was noted. As can be seen from Table 2, decreasing the particle size resulted in an increased rate and completeness of combustion. With the decrease in graphite particle size, the proportion of free valence sites grew as was evident from the increase in oxygen solubility. However, the increase in oxygen content did not seem to inhibit the combustion process.

Among the carbon black powders with approximately the same degree of structural development, increasing oxygen content was

Table 1. Effects of annealing on combustion rate and free carbon content of titanium and carbon powder mixtures, initial C/Ti = 0.967.⁸

Annealing Time (h)	Combustion Rate	Free Carbon
	cm s ⁻¹	
0	2.65	0.05
1	2.34	0.40
4	1.94	0.60

C/Ti = 0.967

Table 2. Graphite particle size effects on combustion.⁸

Particle Size, μm	Combustion Rate cm s^{-1}	Oxygen Content, % In Graphite	Oxygen Content, % In TiC_x	Free Carbon, %	C/Ti x
≤ 30	0.29	0.08	0.6	3.2	0.84
≤ 20	0.38	0.47	0.55	2.1	0.89
≤ 6	1.4	0.51	0.25	0.1	0.95
~ 0.03	1.1	2.2	0.5	0.4	0.92
$\sim 0.1-1$	2.6	0.3	0.18	0.05	0.97

found to decrease the rate and completeness of combustion. Also, the oxygen content in combustion synthesized TiC was approximately proportional to the oxygen content in the starting carbon powder.⁸

Another factor mentioned as a possible influence on the combustion of carbon and titanium powders was the extent that titanium wetted the carbon powder. It was believed that a higher wettability increases the spreading of the molten titanium through the combustion front.⁸

Shkiro, Prokudina, and Borovinskaya⁶ have examined the effects of oxygen content and surface area of titanium powder, sample size, and combustion atmosphere on the synthesis of titanium carbide by the combustion process. For a given surface area of titanium powder, (see Table 3) it was found that the completeness of combustion decreased with an increase in oxygen content. It was also observed that the free carbon content was approximately equal to the oxygen content of the final TiC produced. Also, the final oxygen content was somewhat proportional to initial titanium oxygen content. The effects of titanium powder surface area (when the oxygen content was constant) showed a slight decrease in final oxygen content with an increase in surface area. However, in most cases, increasing the surface area resulted in an increase in sorbed oxygen content of the titanium powder which by far counteracted the advantages incurred by the increase in surface area.

Table 3. Effects of surface area and oxygen content of titanium powders on the resulting titanium carbide.⁶

Ti		TiC _x		
Surface Area m ² /g	Oxy wt%	x	C _{free} %	Oxy wt%
7.123	3.67	0.915	1.4	1.7
5.898	3.63	0.930	1.15	2.05
0.994	5.77	0.770	4.5	4.3
0.724	2.93	0.860	2.0	2.05
0.67	2.32	0.925	0.8	0.95
0.164	0.2	0.950	1.18	0.27
0.233	0.38	0.965	0.1	0.15
0.919	4.45	0.880	1.75	3.1
1.43	2.21	0.905	1.4	1.02

To illustrate the effect of sample size on completeness of combustion Shkiro et al.,⁶ prepared TiC in two sample sizes. The smaller samples weighed approximately 10 g each, and the larger ones 20 kg each. In general there was substantially less oxygen and free carbon in the TiC samples prepared in the 20 kg sizes than those made in the smaller 10 g sizes. For example, samples made from a titanium powder with an oxygen content of 5.77 wt% had final oxygen and free carbon contents of (4.3, 4.5) and (1.35, 1.35) for the smaller and larger sample sizes, respectively.

The importance of maintaining the proper atmosphere during the combustion and cooling periods was also emphasized by Shkiro et al.⁶ Oxygen and carbon monoxide liberated from the combustion zone could react with the sample if not removed quickly. The authors have pointed out that carbon monoxide at the temperatures considered is an oxidizing agent. To illustrate this point, they combusted 10 g samples in argon, and in two carbon monoxide partial pressures. The samples combusted in argon had a final oxygen content of 1.7 wt% compared to 2.7 wt% for a carbon monoxide partial pressure of 0.225 MPa. The starting titanium powder contained 3.67 wt% oxygen. When the same titanium powder was used to combust 20 kg samples with the evolved gases continuously pumped off, the oxygen content was 0.45 wt%.

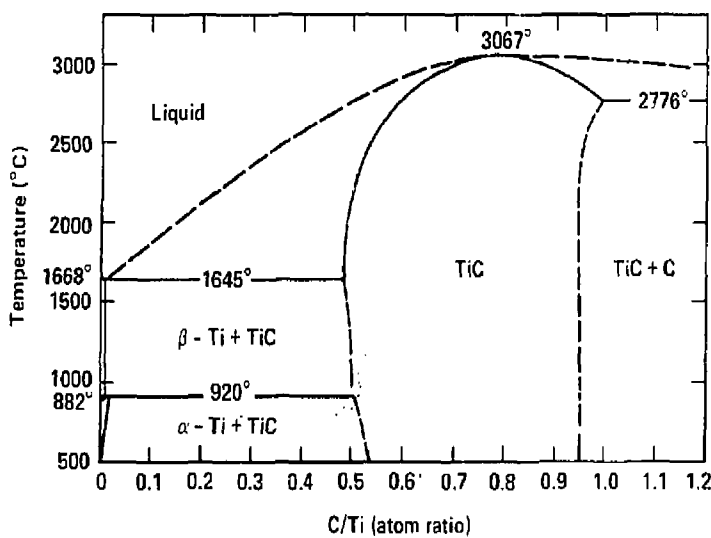
Merzhanov et al.,² have also produced TiC in large (18 to

20 kg) sample sizes. A reaction mixture of titanium and carbon black powders were contained in a water cooled steel vessel. The reaction chamber was evacuated before, and maintained during and after combustion so as to prevent recontamination with evolved gases. The authors did not mention the initial density of the reactants, but according to Shkiro et al.,⁶ compact density is not such a large factor with the bigger sample sizes. The resulting TiC was found to have a combined carbon content of 19.3 to 19.7 wt%, and free carbon and oxygen of <0.3 wt%, and other trace elements totaling no more than 0.25 wt%. Merzhanov et al.² have performed calculations of the adiabatic combustion temperature and have found it to be near the melting point of TiC (3200 K).

A phase diagram for the titanium--carbon system has been presented by Storms.¹⁰ According to this phase diagram (Fig. 1), carbon saturation occurs in TiC at a wt% of carbon of 19.5 (C/Ti = 0.967). At this composition, the melting point is approximately 3163 K. A maximum in the melting point occurs at a composition of 16.5 wt% carbon (C/Ti = 0.785) and is 3340 K.

Few studies have dealt specifically with the sintering of titanium carbide.¹ Most attention has focused on recrystallization and grain growth.¹¹⁻¹⁵ Ordan'yan et al.,¹ have examined the role of stoichiometry in the densification of titanium carbide produced by the SCS process. The powders studied had carbon to titanium atomic ratios of 0.98, 0.87, 0.78, 0.68, and 0.58. Analysis of oxygen content showed the weight percent

Fig. 1 A portion of the Ti-C phase diagram taken from Storms¹⁰.



oxygen to be 0.2 for $TiC_{0.67}$ ($C/Ti = 0.87$), and 0.15 for the other powders. Free carbon decreased with decreasing carbon to titanium ratio. The carbides $TiC_{0.98}$ and $TiC_{0.58}$ had free carbon contents of 0.17 and 0.03 weight percent, respectively. X-ray lattice parameters measurements indicated no difference between $TiC_{0.98}$ to $TiC_{0.68}$ (Ave. 0.4329 nm), but $TiC_{0.58}$ had a value somewhat lower (0.4312 nm). Uncertainties in these measurements were not given. After milling, the powders had an average surface area of $5 \text{ m}^2/\text{g}$.

Densification of sintered pellets was found to depend on stoichiometry in such a way that lower total carbon content produced higher sintered densities. Grain size measurements showed that after sintering for 60 min. at 1770 K, the mean grain size of $TiC_{0.98}$ and $TiC_{0.58}$ were approximately 10 μm and 40 μm , respectively. Thus grain growth is also substantially dependent on stoichiometry. Estimation of the activation energies for the various powders revealed a trend with stoichiometry. Values for activation energy, as shown in Table 4, were found to vary from 468 to 293 KJ/mole for $TiC_{0.98}$ to $TiC_{0.58}$, showing a decrease with decreasing C/Ti ratio. The conspicuous absence of kinetic plots (logarithm shrinkage versus logarithm time) and the statement of using a holding time of one hour, and no other times, for sintering at various temperatures, leads one to believe that kinetic experiments were not performed by Ordan'yan et al.¹ Without knowledge of the sintering kinetics, the activation

Table 4. Sintering Activation Energy, Q, for TiC_x

<u>X</u>	<u>Q (kJ/mole)</u>
0.58	292
0.68	297
0.78	313
0.87	422
0.98	468

energies can not be calculated, and any estimation of them ignoring the kinetics will be erroneous.

Chermant et al.,¹¹ studied the final stage of sintering as well as grain growth in titanium carbide. One of the powders used was obtained from the Starck Chemical Co. and had an average particle size of 75 nm (750 Å). It was noted that the final stage of sintering was controlled by grain boundary diffusion and above 2173 K rapid grain growth takes place which impedes the sintering process. Several other workers¹²⁻¹⁵ have noted similar grain growth patterns. Samsonov and Bozhko¹³ observed the effects stoichiometry had on recrystallization and grain growth in TiC. In general, a lower carbon to titanium ratio resulted in faster grain growth. For example, after sintering at 2273 K for two hours, compacts with a starting particle size of 3 μ m had an average grain size of 8 and 15 μ m for $TiC_{0.96}$ and $TiC_{0.58}$, respectively. There also appeared to be a temperature dependence on the limiting grain size, again with the same stoichiometry dependence.

In plots of the logarithm grain size versus inverse temperature there was a trend in which the carbides with lower C/Ti ratios have a lower slope. Samsonov and Bozhko¹³ have determined activation energies for the various stoichiometries from the Arrhenius plots mentioned above. The activation energies were 187, 138, 149, 98.6 kJ/mole (44.8, 33.0, 35.6, 23.6 kcal/mole) for C/Ti ratios of 0.96, 0.86, 0.80 and 0.58,

respectively. There was no mention of the rate controlling mechanism, but according to Kingery¹⁶ the activation energy of grain growth should be between that of boundary and lattice diffusion. As will be shown later, the activation energy for lattice self-diffusion of titanium and carbon in $TiC_{0.97}$ are 737 and 398 kJ/mole respectively. Grain boundary diffusion is usually about one half that of lattice diffusion (368 for Ti and 196 kJ/mole for C). The activation energy determined by Samsonov and Bozhko¹³ compares reasonably well with the estimated grain boundary activation energy for carbon diffusion.

Kushtalova¹² has studied the sintering of loosely poured TiC powder with composition 80.2 wt% Ti 18.8 wt% C total (C/Ti = 0.936) and 0.04 wt% free C. The average particle size was 8.5 μm . Sintering was performed over the temperature range 1673 K to 2373 K under a vacuum of 0.13 Pa (10^{-3} Torr) with a heat-up time of one hour. After holding for two hours at 1773 K, the mean grain size had increased to 17 μm diameter. Rapid grain growth was observed at temperatures approaching 2073 K and above. At 2173 K a fairly strong, highly porous (50%) compact was formed. From a plot of $\ln d^2$ vs $1/T$ (d = grain diameter T = Temperature in K) the activation energy for grain growth was found to be 242 \pm 6.3 kJ/mole. This value is reasonably close to that found by Samsonov and Bozhko,¹³ 187 kJ/mole.

The effects of annealing on the composition and structure of TiC were examined by Vavrda and Blazikova.¹⁵ The TiC considered

had a C/Ti ratio of 0.961 (combined carbon) with a free carbon content of 0.29 wt%. To examine the effects of annealing atmosphere on the lattice parameters of TiC, specimens were heated for three hours at 1573 K in purified hydrogen; in a vacuum of 1.3 Pa (10^{-2} Torr) and $1.3 \times 10^{-2} \text{ Pa}$ (10^{-4} Torr); and in purified argon. A decrease in the lattice parameter was observed for heat treatment in hydrogen and vacuum, while an increase was observed for argon heat treatment (initial parameter 0.43262 nm, 0.43240 nm in hydrogen, 0.43249 nm vacuum, 0.43272 nm in argon with an average uncertainty of ± 0.0006 nm). According to Costa and Conte¹⁷ the lattice parameter of TiC decreases with decreasing carbon to titanium ratio (see Table 5). The above results thus indicate some decarburization occurs during heat treatment in hydrogen and vacuum.

Changes in particle morphology were studied for annealing temperatures of 1573, 1873, 2073, and 2273 K in argon for one hour. At 1573 and 1873 K no changes were observed. However, at 2073 K sintering of fine particles ($> 2 \mu\text{m}$) to larger ones ($10-20 \mu\text{m}$) became noticeable, and at 2273 K bonds were formed between large particles.

The volume self-diffusion coefficients of carbon in TiC with C/Ti ratios of 0.97, 0.89, 0.67, and 0.47 were determined by Sarian^{18,19} and by Bremeev and Panov.²⁰ Sarian's results are

$$D_{0.97} = (6.98 \pm 1.24) \exp(-[398 \pm 3]/RT) \text{ cm}^2/\text{sec}$$

$$D_{0.89} = (45.44 \pm 5.12) \exp(-[446 \pm 1.6]/RT) \text{ cm}^2/\text{sec}$$

Table 5. Lattice Parameters, a , of TiC_x^{17} .

<u>x</u>	<u>a (nm)</u>
0.5	0.42990 ± 10^{-4}
0.6	$0.43120 \pm 5 \times 10^{-5}$
0.7	0.43215 ± 10^{-4}
0.8	$0.43250 \pm 5 \times 10^{-5}$
0.9	$0.43290 \pm 5 \times 10^{-5}$

$$D_{0.67} = (114 \pm 66) \exp(-[459 \pm 8.4]/RT) \text{ cm}^2/\text{sec} .$$

Bremeev and Panov's result is

$$D_{0.47} = 190 \exp(-462/RT) \text{ cm}^2/\text{sec} .$$

The activation energies are in kJ/mole.

Sarian²¹ also determined the self-diffusion coefficient of titanium in TiC. It was found to be $D = 4.36 \times 10^4 \exp(-[737.3 \pm 15]/RT) \text{ cm}^2/\text{sec}$, and was not dependent on stoichiometry.

Sarian¹⁹ has suggested that the stoichiometry dependence of carbon diffusion in TiC is due to short range ordering of the carbon vacancies. It should be noted that the activation energies measured by Sarian^{18,19,21} and by Bremeev and Panov²⁰ show a different dependence on stoichiometry than the sintering results of Ordan'yan et al.¹

II. Materials and Methods

A. Powder Preparation

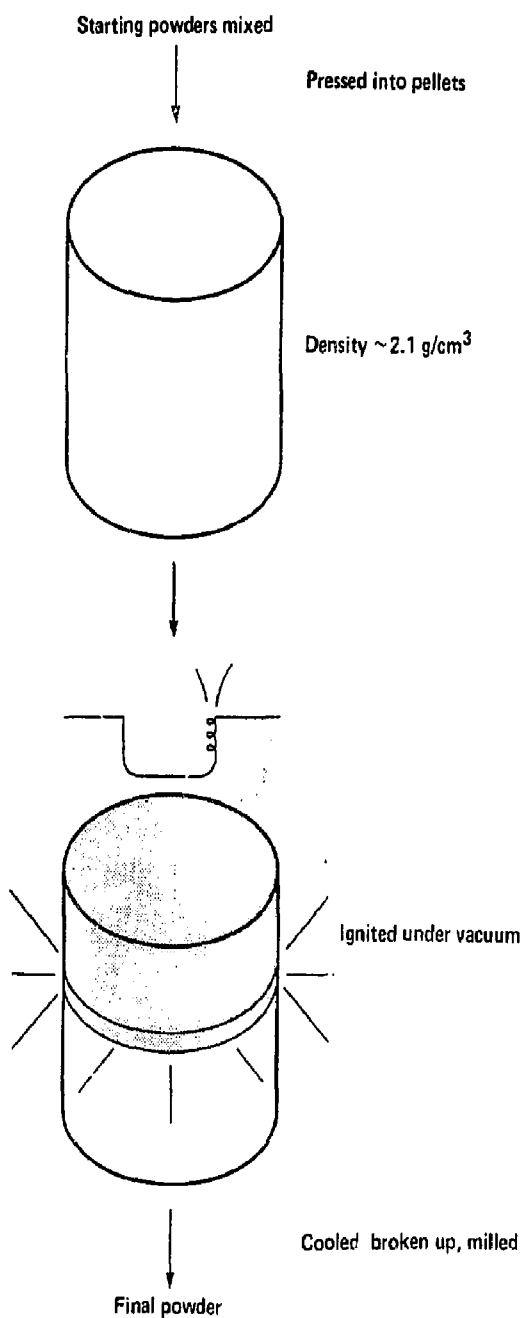
Eight preparations of TiC were used in this study: one obtained from the Starck Chemical Company (C/Ti = 0.956), and the other seven made in this investigation using the self-propagating high-temperature synthesis (SBS) process described by Merzhanov and Borovinskaya.⁶

The seven SBS samples of TiC (labeled as SYN 1 through 7) were made as follows. SYN 1 was made from titanium powder of -325 mesh obtained from Alfa Products, and carbon powder (graphite form) of -325 mesh obtained from Union Carbide Corporation. The

titanium and carbon powders were combined in the ratio 19.0 wt% carbon and 81 wt% titanium for a nominal C/Ti ratio of 0.936, and then mixed for twenty minutes in a Spec mechanical shaker. This particular ratio of carbon to titanium was chosen to be slightly below the maximum possible ratio (C/Ti = 0.967) which would yield a single-phase product if completely combusted. Some titanium was lost during the combustion process as indicated by the resulting TiC having a stoichiometry slightly higher than what was started with. The mixture was then loosely packed in a graphite crucible 3.81 cm ID and 5.08 cm high. The crucible with the reaction mixture was subsequently placed in a vacuum box and pumped down to a pressure of 0.2 Pa. Ignition of the powder mixture was achieved via a tungsten coil of 1.5 cm diameter, approximately 3 millimeters above the mixture, with a current of 65 amp. After combustion, the composition was found to be 19.28 wt% by weight carbon, 80.72 wt% titanium (C/Ti = 0.953). The total carbon content was determined by oxidizing the TiC and measuring the weight of CO_2 evolved.

Samples designated as SYN 2 were prepared using the same reaction mixture as SYN 1, but the mixture was pressed into a pellet before ignition. Figure 2 shows a schematic of this process. The pellets weighed 15 grams each and were 1.95 cm in diameter. They were pressed under a load of 2 kN and had a density of 2.1g/cm^3 . After combustion the C/Ti ratio was determined as 0.955.

Fig. 2 The combustion process of titanium and carbon used for SYN 1 and 2 powders.



SYN 3 samples were the same as SYN 2 except that the pellets were baked out in a vacuum furnace at 1223 K for 12 hours and then ignited by raising the temperature of the pellet at approximately a rate of 60 K per minute until ignition took place at 1873 K \pm 50 K, as measured with an optical pyrometer. The final composition was determined with a C/Ti = 0.950.

SYN 4 was the same as SYN 3 except there was no bake out period. The temperature was raised from room temperature at a rate of 60 K per minute until ignition took place at approximately 1873 K. The final composition was determined as C/Ti = 0.954.

SYN 5 was prepared from a mixture of 18.38 wt% carbon, and 81.62 wt% titanium hydride (i.e., an initial C/Ti of 0.936). The combustion conditions were the same as those for SYN 3. The final C/Ti ratio was 0.951.

SYN 6 was prepared under the same condition as SYN 1 except that the composition was 17.51 wt% carbon, 82.49 wt% titanium (initial C/Ti of 0.847). The final C/Ti ratio was 0.858.

SYN 7 was prepared under the same conditions as SYN 5 except the C/Ti ratio was 14.41 wt% carbon and 85.59 wt% titanium hydride (initial C/Ti of 0.70). After combustion the composition was found to correspond to a C/Ti of 0.703.

A summary of the reaction conditions is shown in Table 6 along with the initial and final C/Ti. Figure 3 shows a polished and etched micrograph of a typical pellet after combustion. The density of this pellet was 55%.

Table 6. Summary of Combustion Conditions for SYN Powders.

SYN 1 Combusted from loose powders of (Ti + C) in a glovebox. Initial C/Ti = 0.936, final C/Ti = 0.953.

SYN 2 Combusted from pressed pellet of (Ti + C) powders in a glovebox. Maximum density 2.1 g/cm³. Initial C/Ti = 0.936, final C/Ti = 0.955.

SYN 3 Combusted from pressed pellet of (Ti + C) powders in a furnace after baking out \sim 12 hours at 1223 K (under vacuum of $\sim 10^{-4}$ Pa). Heating rate up to combustion was 60 K/min. Ignition at \sim 1873 K. Combustion temp 2523 ± 50 K initial C/Ti = 0.936, final C/Ti = 0.950.

SYN 4 Same as SYN 3, but no bake out, final C/Ti = 0.954.

SYN 5 Same as SYN 3, but used (TiB + C), final C/Ti = 0.951.

SYN 6 Same as SYN 1, except Initial C/Ti = 0.800, final C/Ti = 0.858.

SYN 7 Same as SYN 5, except Initial C/Ti = 0.700, final C/Ti = 0.703.



Fig. 3 An etched micrograph of a typical pellet after combustion, mag. 500X.

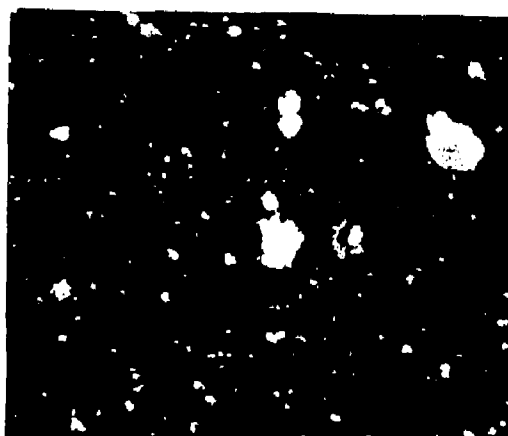


Fig. 4 SEM of SYN 1 powder after milling 24 h. The half width of the photo is 10 μ m.

After cooling the combusted samples to room temperature, they were broken up using a boron carbide mortar and pestle, and then milled in a tungsten carbide vibratory ball mill in 20 g batches until the desired surface area was attained. The surface areas of the powders were measured by the BET method using a surface area analyzer (model number 2100A) from Micrometrics Instrument Corporation. X-ray diffraction was used to determine the lattice parameters of the commercial (Starck), SYN 1, SYN 5, and SYN 7 powders. The Nelson-Riley²² extrapolation function was used to analyze the Debye-Scherrer patterns. The lattice parameters obtained are listed in Table 7. The results of spectrochemical analysis performed at Lawrence Livermore National Laboratory (LLNL) are shown in Table 8. Pycnometric densities of the powders were measured using an He-air pycnometer are shown in Table 9. The pycnometer was designed and built at LLNL.

Figure 4 is a scanning electron micrograph of the SYN 1 powder milled for 24 hours. In the background are 0.1 μm holes of a nutropore filter. The wide distribution of particle sizes and groups of agglomerates were typical of the powders. A scanning electron micrograph of a polished sintered pellet of SYN 1 (density 84%) is shown in Fig. 5. The bright spots were identified as regions of high tungsten concentration, apparently flakes chipped off the WC ball mill during milling.

B. Pellet Preparation

Pellets for sintering were pressed under atmospheric

Table 7. Lattice parameters of TiC_x .

Sample	$\text{\AA} (\text{nm})$
SYN 1	0.4327 ± 0.0004
SYN 5	0.4324 ± 0.0004
SYN 7	0.4316 ± 0.0003
Starck	0.4330 ± 0.0001

Table 8. Spectrochemical Analysis of Commercial* and SYN 1 Powders after milling 24 hours (in wt%).

Impurity	Commercial Powder	SYN 1 Powder
W	0.6	0.4
Al	0.03	1.0
Fe	0.01	0.02
Ca	0.003	0.2
Cr	0.003	0.0003
Mg	0.006	0.001
Mn	0.001	0.01
Nb	0.003	0.003
Si	0.0005	0.06
Ni	-	0.001
Sr	-	0.003

*Starck Chemical Co.

Table 9. Pycnometric density (g/cm^3) of TiC powders after milling 30 minutes.

Sample	Density (g/cm^3)
Commercial*	4.91
SYN 1	4.64
SYN 2	4.79
SYN 3	4.88
SYN 4	4.80
SYN 5	4.91
SYN 6	4.69
SYN 7	4.76

*Starck Chemical Co.

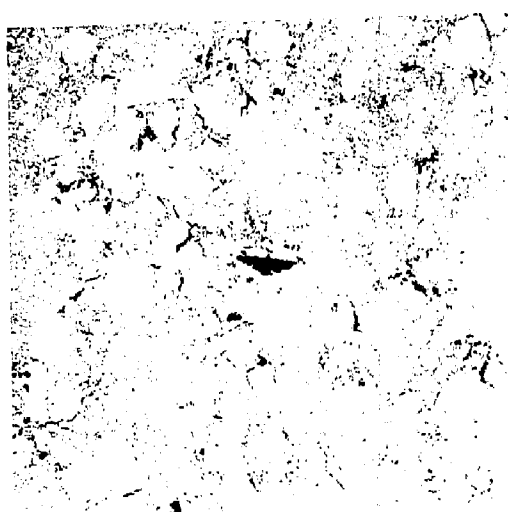


Fig. 5 SEM of polished sintered pellet of SYN 1.

conditions in a double action steel die with 0.645 cm diameter pistons. The average load applied was 1 kN (3×10^4 Pa).

Stearic acid was used to lubricate the die walls and pistons to aid in compaction and removal of the pellets from the die. The resulting pellets had average densities of 65.6 ± 0.4 % of theoretical for the commercial and SYN 1, and 68.1 ± 0.3 for SYN 5, and 67.2 ± 0.5 for SYN 7, and typical dimensions of 0.930 cm long, 0.645 cm dia. Before sintering, the pellets were weighed to the nearest 0.001 g and measured to the nearest 0.002 cm. These measurements were repeated after sintering.

C. Sintering

Sintering was performed in a Brew vacuum furnace in the pressure range 1.3×10^{-3} to 1.3×10^{-4} Pa (10^{-5} to 10^{-6} Torr). The temperature was measured with an optical pyrometer with an accuracy of ± 10 K. A heating rate of 20 K per minute was used to bring samples up to 1273 K (50 min) and then changed to 30 K per minute until the sintering temperature was reached. Samples were held at the sintering temperature for times ranging from 60 to 1020 minutes. Sintering temperatures were between 1423 K and 1873 K. For the Arrhenius plots of logarithm shrinkage versus inverse temperature, a sintering time of 60 minutes was used. Kinetic and Arrhenius plots were determined for the commercial, SYN 1, SYN 5, and SYN 7 powders. The powders had surface areas of 13.6, 12.4, 6.52 and $9.91 \text{ m}^2/\text{g}$ respectively.

Comparison of the shrinkages of the commercial and SYN

powders 1 through 6 were made at a temperature of 1813 K for a time of 60 minutes. The powder surface areas were approximately $4 \text{ m}^2/\text{g}$, and the exact values are shown in the results.

Carbon powder was added to the commercial material to examine the effects of free carbon on sintering. The amounts of carbon added to 15 g of commercial TiC were 0.25, 0.10, 0.05, 0.02 and 0.011 g. All five carbon-doped samples plus one undoped sample were milled in 15 g batches for one hour in a WC vibratory ball mill. Pellets prepared from these powders were subsequently sintered at temperatures of 1723 K and 1843 K for 60 minutes. In addition to the above samples, one was prepared by adding 0.469 g of carbon to 15 g of commercial TiC, and milled for 24 hours (surface area $13 \text{ m}^2/\text{g}$). Pellets from this sample were sintered at 1541 K for 60 minutes along with SYN 1, and undoped commercial powder.

III. Results

Plots of the natural logarithm of the fractional volume shrinkage vs. the natural logarithm of isothermal sintering time for several temperatures are shown in Figs. 6 through 9 for the commercial, SYN 1, SYN 5, and SYN 7, respectively. The slopes of these plots are related to the mechanism characteristic exponent, m , from the equation¹⁵

$$\Delta V/V_0 = (K D_0 t \exp[-Q/RT])^m \quad (1)$$

where Q is the activation energy for diffusion, $D_0 \exp[-Q/RT]$ is the diffusivity, K is a function of material constants and

Fig. 6 $\ln \Delta V/V_0$ vs $\ln t$ for commercial pellets.

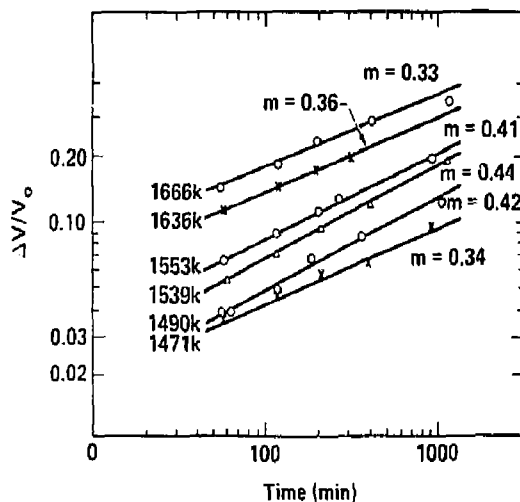


Fig. 7 $\ln \Delta V/V_0$ vs $\ln t$ for SYN 1 pellets.

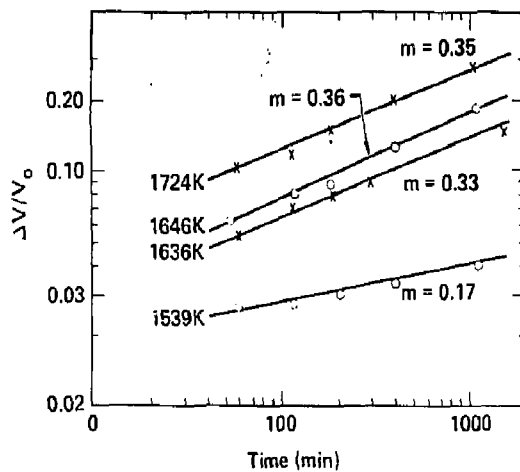


Fig. 8 $\ln \Delta V/V_0$ vs $\ln t$ for SYN 5 pellets.

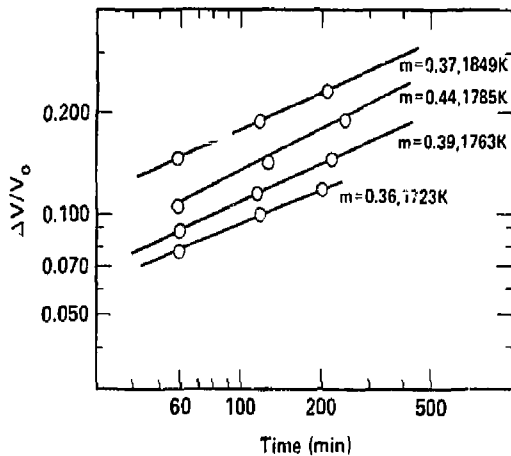
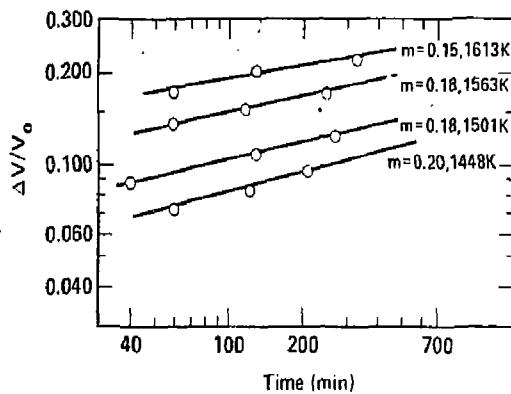


Fig. 9 $\ln \Delta V/V_0$ vs $\ln t$ for SYN 7 pellets.



temperature, t is the isothermal sintering time, and $\Delta V/V_0$ is the fractional volume shrinkage. According to Johnson and Cutler,²³ m is related to the rate controlling mechanism for the sintering process. The average m values for the slopes given in Figs. 6 through 9 are (excluding the low slope for SYN 1 in Fig. 7) 0.38 ± 0.02 , 0.34 ± 0.01 , 0.39 ± 0.02 , and 0.18 ± 0.02 for the commercial, SYN 1, SYN 5 and SYN 7, respectively.

Figures 10, 11, and 12 show plots of the $\ln \Delta V/V_0$ versus inverse temperature for a time of 60 minutes for the commercial and SYN 1 (both in Fig. 10), and SYN 5 (Fig. 11), and SYN 7 (Fig. 12). Activation energies for the sintering process were calculated using the slopes of these Arrhenius plots and the average m values from the $\log \Delta V/V_0$ versus $\log t$ kinetic plots. These activation energies were 389 ± 20 , 458 ± 13 , 376 ± 20 , and 492 ± 25 kJ/mole for the commercial, SYN 1, SYN 5 and SYN 7, respectively. It is significant that the activation energies for the SYN 1 and SYN 7 are notably higher than those of SYN 5 and the commercial powder. The data for the above kinetic and Arrhenius plots are shown in the appendix.

The results of sintering the commercial and SYN powders 1 through 6 are shown in Table 10. For ease of comparison, the pycnometric density, surface area, and oxygen content of each powder are also shown. From this table it can be seen that in general the sinterability of the powders increases with increasing pycnometric density and decreasing oxygen content.

Fig. 10 $\ln \Delta V/V_0$ vs $10^4/T$ for commercial and SYN 1 pellets.

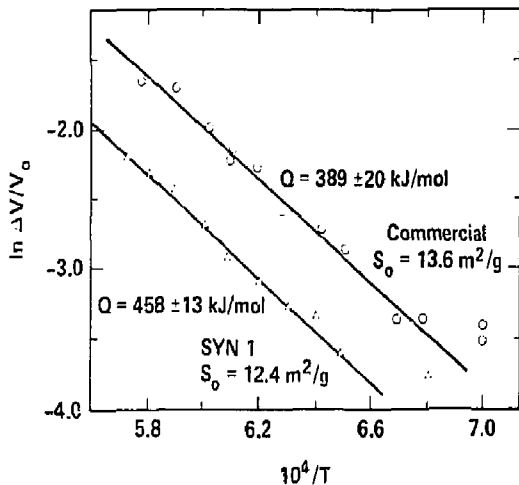


Fig. 11 SYN 5 ($\text{TiH}_2 + \text{C} \rightarrow \text{H}_2 + \text{TiC}$) $S_0 = 6.52 \text{ m}^2/\text{g}$.

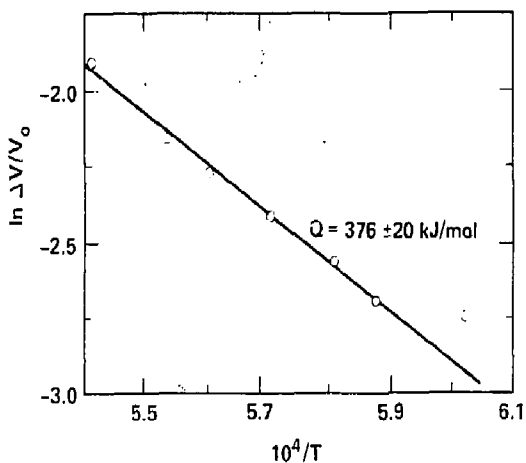


Fig. 12 $\ln \Delta V/V_0$ vs $10^4/T$ for SYN 7 pellets.

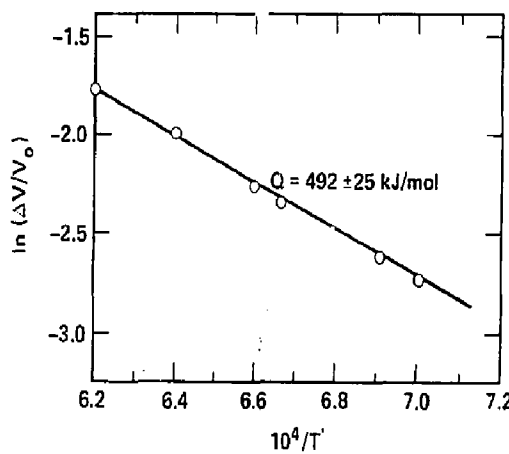


Table 10. Sintering Data of SYN 1-6 and Commercial Powders at 1813 K for 60 minutes.

Material	$\Delta V/V_0$	Pycnometric Density (g/cm ³)	S_O (N ² /G)	Wt% Oxygen
	± 0.003	± 0.005	$\pm ?$	$\pm ?$
SYN-1	0.000	4.64	3.75	--
SYN-2	0.011	4.79	3.72	0.88
SYN-3	0.064	4.88	3.81	1.20
SYN-4	0.053	4.80	3.85	0.66
SYN-5	0.068	4.91	3.91	1.96
SYN-6	0.221	4.69	3.29	--
Commercial	0.219	4.91	4.02	0.45

This relationship will be touched upon in more detail in the discussion section. It is also apparent that commercial TiC powder exhibits a higher degree of shrinkage than all the near stoichiometric SYN powders (SYN 6 is non-stoichiometric).

Table 11 contains the results of sintering the commercial material to which had been added varying amounts of carbon. From these results, it is concluded that free carbon inhibits the shrinkage of compacts of TiC. To analyze the effect of free carbon dispersion within the TiC compact 0.469 g of carbon was added to 15 g of Starck TiC and subsequently milled to an approximate surface area of $13 \text{ m}^2/\text{g}$, and then sintered at 1814 K for 60 minutes along with samples of SYN 1 ($S = 12.4 \text{ m}^2/\text{g}$) and commercial (no added carbon, $S = 13.6 \text{ m}^2/\text{g}$). The resulting volume shrinkages were 2.5%, 2.6%, and 5.6% for the commercial powder with added carbon, SYN 1, and commercial powder (no added carbon), respectively. Thus, increasing the milling time of commercial TiC with carbon powder added decreases the relative difference in sintering shrinkage observed between SYN 1 and commercial powders.

IV. Discussion

It is apparent from the results shown in Table 10 that the stoichiometric SYN powders 1-5 exhibit lower shrinkage rates during sintering than the commercial TiC. To probe the possibility that incomplete combustion of the SYN materials was a

Table II. The effect of carbon additions on the sintering of Commercial TiC^a.

% of Total Carbon Free	$\frac{\Delta V}{V_0}$	
	T = 1843 K	T = 1723 K
14.00	0.128	0.108
6.50	0.160	0.128
3.28	0.190	0.133
1.32	0.237	0.143
0.66	0.252	0.146
No carbon added	0.303	0.151

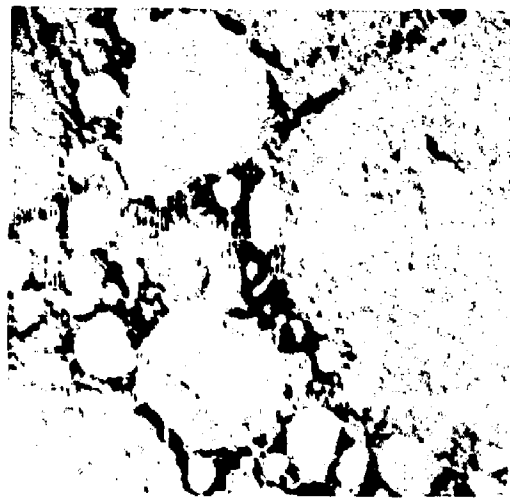
a) Carbon added to Starck material

b) Error in $\frac{\Delta V}{V_0} \sim 0.003$

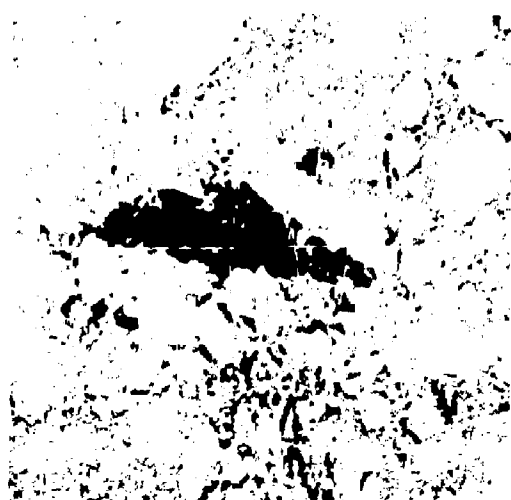
major cause of the difference in the sintering behavior between the commercial and SYN materials, qualitative tests for free titanium and free carbon were performed. Analysis for dissolved titanium in an acid solution showed negative results, however, a film of carbon powder was noted on the liquid's surface.

Merzhanov et al.,² have also observed floating carbon films during washing of SHS produced TiC. Direct measurement of the free carbon content of the powder by dissolving away the titanium carbide phase proved inadequate for quantitative determination of free carbon content, but did show qualitatively that free carbon was present in all the SYN powders to a larger degree than the commercial powder. X-ray diffraction results also indicated some free carbon in the SYN 1 powder. Using the elemental identification mode on a scanning electron microscope, several attempts were made at finding free carbon or carbon rich phases in sintered samples of SYN 1 and commercial TiC. Figure 13 shows typical micrographs resulting from this technique. The bright horizontal line is the region scanned, and the high peak in the center is a region of high carbon concentration. During analysis of such micrographs, no discernible difference between SYN 1 and commercial polished pellets were detected. It was therefore concluded, in light of what follows, that diamond used in the polishing of the samples had lodged in the cracks and voids and thus prevented any meaningful interpretations from being made.

Nezhevenko, Groshev, Gurevich, and Bokov⁷ have analyzed



(a) Commercial



(b) SYN 1

Fig. 13 Polished sintered pellets of commercial (a) and SYN 1 (b). The sintering temperature was 1973K.

the free carbon contents of ZrC powders and have reported these free carbon contents along with the pycnometric density and oxygen contents of the powders, see Table 12. Their results indicated a relationship between the pycnometric density, oxygen, and free carbon content. The following two trends were notable: with an increase in free carbon content the pycnometric density went down; for a given free carbon content, increasing the oxygen content increased the density.

A semi-quantitative estimate of the free carbon content of the powders by assuming a two-phase system (C + TiC) was performed. The TiC phase was assumed to have a complete titanium sublattice and an incomplete carbon sublattice. The amount of free carbon was estimated for each powder using the lattice parameters determined by x-ray diffraction, the measured pycnometric density, and the known density of graphite. After examination of Table 3, it was assumed that the amount of oxygen in the sample displaces an equivalent amount of carbon from the lattice in addition to what was calculated above. In all the TiC samples, the total amounts of carbon and titanium were known. The oxygen content was known in samples SYN 2, 3, 4, 5 and the commercial TiC.

The calculation showed that 14-17% of the carbon in the SYN 1 material was free (assumed oxygen content was 1% by weight). The range of estimated free carbon is due to the uncertainty in the lattice parameters of the TiC phase, and in the density of

Table 12. Chemical Composition and Pycnometric Density for ZrC.⁷

Zr	Chemical Composition wt%			Pycnometric density (g/cm ³)
	C _{total}	C _{free}	Oxy	
78.5	14.4	6.71	7.0	4.83 - 5.10
87.1	11.3	1.0	2.0	5.77 - 5.80
88.7	10.6	0.1	0.4	5.93 - 6.20
88.8	10.8	0.1	0.2	5.79 - 6.20

graphite. The free carbon content of the SYN 2 material was calculated to be 8-9% of the total carbon. Since the only difference between the SYN 1 and SYN 2 production methods was the initial bulk density of the materials, (SYN 1 was loose, SYN 2 had a 2.1 g/cm^3 bulk density) the difference in the free carbon contents must be due to this difference in initial bulk density. Merzhanov and Borovinskaya³ have noted this phenomenon, as well as Sarkisyan et al.⁴

The possible effects of sorbed gases in the starting materials and of heat conductivity away from the reaction mixture were investigated using the experimental procedures outlined for the production methods of SYN 3, 4, and 5. SYN 3 and 4 were combusted from pellets indentical to those used in the combustion of SYN 2, except SYN 3 pellets were outgassed at 1223 K for 12 hours before combustion, and SYN 4 did not have this bake out period. Combustion took place in a vacuum furnace by raising the temperature at 60 K per minute until combustion took place at 1873 K. During combustion, little outgassing was observed with the SYN 5. However, substantial outgassing as evidenced by an increase from 10^{-3} to 10^3 Pa in the vacuum with the SYN 4 material. It should be noted here that the pycnometric densities and oxygen contents of these two powders differed significantly; SYN 3 (4.88 g/cm^3 , 1.2 wt% O_2) and SYN 4 (4.80 g/cm^3 , 0.66 wt% O_2). The calculated free carbon contents were 6 - 7% of the total carbon for each powder. However, it is believed that

the SYN 3 has a lower free carbon content. The reason for the apparent equality in the calculated free carbon values is that the oxygen contents differ by almost a factor of two and 1 weight percent oxygen was assumed to displace 3% of the carbons from their lattice sites. The validity of the above assumption is supported by the observations of Shkiro, Prokudina, and Borovinskaga⁶ on the relationship between free carbon content to oxygen content in combustion synthesized TiC, shown in Table 3, in which the free carbon content was approximately equal to the oxygen content of the TiC produced.

To further explore the role of outgassing in the combustion synthesis process, titanium hydride powder was used in the synthesis of SYN 5 instead of titanium metal powder. Pellets pressed from a mixture of titanium hydride and carbon powders were baked out at 773 K under a vacuum of 1.3×10^{-3} Pa (10^{-5} Torr) until outgassing caused by decomposition of the hydride stopped, after which the samples were baked out at 1223 K for 12 hours before ignition. During combustion, no outgassing was observed. The resulting high-pycnometric density (4.91 g/cm³) was expected. However, the high oxygen content (1.96 w/o O₂) was not. Calculating the free carbon content caused by the oxygen displacement of carbon gives 5-6% of the total carbon free.

Table 13 shows the estimated free carbon contents of the SYN 1-5 and commercial TiC samples. For comparison, the shrinkages of pellets pressed from these powders and sintered at 1813 K for

Table 13. Comparison of Calculated Free Carbon to Volume Shrinkage After Sintering at 1813 K.

Material	Calculated % Free Carbon	$\Delta V/V_0 \pm 0.003$
SYN 1	14-17	0.000
SYN 2	8-10	0.011
SYN 3	6-7	0.064
SYN 4	6-7	0.053
SYN 5	5-6	0.068
Commercial	< 2	0.219

60 minutes are shown. Comparing the shrinkage to free carbon content, it is apparent that free carbon has inhibited the sintering of the combustion synthesized TiC. The results of adding carbon powder to the commercial TiC, shown in Table 11 and the examination of the effect of free carbon dispersion on sintering TiC, substantiate this conclusion.

In Figs. 14 and 15 are shown the grain structures of the commercial and SYN 1 carbides after sintering at 1816 K for 60 minutes (relative densities 91 and 83%). Both are characterized as having regions of large grains within smaller grains. However, this is more pronounced in the commercial material than in SYN 1. In addition, the grains of the commercial material appear approximately a factor of two larger than the SYN 1. Although a detailed examination of grain growth was not performed in this experiment, it appears reasonable that free carbon which has inhibited sintering has also retarded grain growth.

The difference detected between the activation energies of the commercial and SYN 1 carbides can also be ascribed to the incomplete combustion of the SYN 1 TiC. During chemical analysis of the SYN 1 product, no free titanium was found, while free carbon was abundant. This means that the TiC phase in the SYN 1 powder was carbon deficient. Furthermore, the activation energies for the sintering of ZrC^{24-26} , ZrN^{26} , NbC^{27} , TiN^{28} , and TiC^1 are known to be dependent on stoichiometry. In all the above mentioned materials, except NbC^{27} and TiC^1 ,

— 20 μ m



Fig. 14 SYN 1 pellet sintered at 1816K for 1h. Density was 83%, magnification 1000X.

— 20 μ m



Fig. 15 Commercial pellet sintered at 1816K for 1h. Density was 91%, magnification 1000X.

a decrease in carbon or nitrogen content increases the activation energy. For the cases of NbC^{27} and TiC^1 , Ordan'yan et al.,^{1,27} did not mention the time dependence of shrinkages during sintering. Such an approach ignores the possible temperature, particle size, stoichiometry, and other physical or chemical dependencies of the m value in Eq. (1). The results obtained in this experiment indicate a substantial dependence of m on stoichiometry. *SYN 7* with $C/Ti = 0.703$ had $m = 0.18$, while commercial TiC with $C/Ti = 0.957$ had $m = 0.38$. If an m value of 0.38 was used, however, in the calculation of the activation energy for the *SYN 7* TiC , the resulting activation energy would be 233 kJ/mole and would agree qualitatively with the results of Ordan'yan et al., for TiC^1 and NbC^{27} . Thus the high activation energy determined for the *SYN 1* TiC is interpreted as being caused by a nonstoichiometric carbide lattice.

In sintering the rate controlling mechanism is often determined by comparison of the measured m values of Eq. (1) to the m values predicted from theory. The average m values measured in this experiment for the commercial and *SYN 5* materials (0.38 and 0.39, respectively) correspond to the predicted mechanism of volume diffusion. However, the average m value obtained for *SYN 1* was low (0.34), and that obtained for *SYN 7* much lower yet (0.18). The m value of 0.34 for *SYN 1* could be explained as being caused by grain boundary diffusion or simply experimental error. But, the exceptionally low value

obtained for SYN 7 ($C/Ti = 0.703$) cannot be explained so simply, and clearly more experimental data are needed on the stoichiometric dependence of the m value before a meaningful explanation can be given. Grain growth appears to be the most plausible explanation for the low m values. In attempting to measure grain growth, polishing of samples below a density of 85% proved to be impossible because the grains would tear out of the samples.

Assuming that the trend in activation energy with stoichiometry determined in this experiment is correct, comparison with the measured volume self-diffusion activation energies of carbon¹⁸ and titanium²¹ in TiC and their dependencies on stoichiometry supports the proposition that the controlling mechanism for sintering TiC is carbon volume diffusion. This same phenomenon has been noted by Andrievskii et al.,²⁶ for the sintering of ZrN. They observed a trend in activation energies calculated from sintering experiments on the neck growth rates between ZrN wires. For this case a decrease in nitrogen content resulted in a decrease in the sintering rate and an increase in the calculated activation energy.

It should be noted that the opposite phenomenon (higher sintering rates with lower carbon contents) is observed in the sintering of powder compacts of ZrC²⁴⁻²⁶, NbC²⁷, TiN²⁸, ZrN²⁶ and TiC.¹ In this experiment, nonstoichiometric TiC (SYN 6 with $C/Ti = 0.854$ and SYN 7 with $C/Ti = 0.703$) also exhibited enhanced shrinkage. However, this does not necessarily

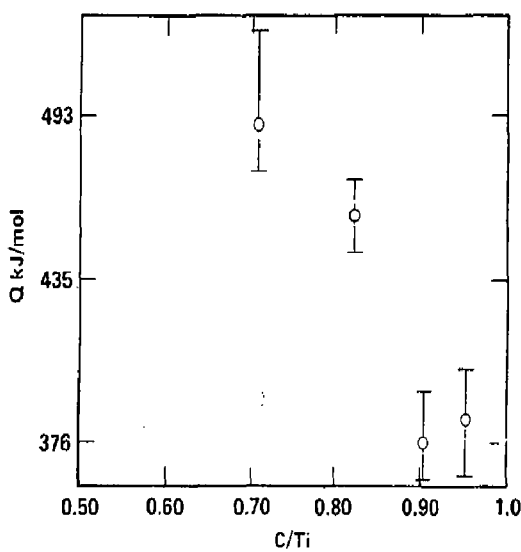
contradict the findings of Andrievskii et al.,²⁶ because the wires used by these workers were relatively free from the stresses and strains which are present in the powder form. According to Kravchik et al.,²⁹ the deformation characteristics of NbC varies with stoichiometry, as was readily seen from the variation in specific surface area with milling time for powders of different compositions. In general, NbC near the stoichiometric composition milled to a higher surface area in less time than the powders with a lower carbon content. Such variations in the mechanical properties with stoichiometry could account for the difference in the sintering rates between stress-free wires (and spheres) and powder compacts of ZrC, and ZrN.

V. Summary

Free carbon in the combustion synthesized TiC was found to be the cause of a reduced sintering rate when compared to the commercial TiC which had much less free carbon. The value of the coefficient of the time dependence of shrinkage, m , was found to be dependent on stoichiometry and thus prohibited efforts to determine the sintering mechanism by comparing the measured m values to those determined by theory. For a C/Ti ratio of 0.956 and 0.703 the m values were 0.38 ± 0.02 and 0.18 ± 0.02 respectively.

Assuming equation (1) to be applicable to the sintering of nonstoichiometric TiC, activation energies were calculated. Figure 16 shows the dependence of activation energy, Q , on C/Ti

Fig. 16 Dependence of activation, Q , on C/Ti .



of the TiC phase ($C_{TiC} = C_{total} - C_{free}$). From this plot it is clear that Q increases with decreasing C/Ti in the TiC phase. Comparing the C/Ti dependence, and magnitudes of the activation energies measured in this experiment with the activation energies for self diffusion of carbon and titanium in TiC leads to the conclusion that carbon diffusion is the rate controlling mechanism for sintering of TiC.

ACKNOWLEDGEMENTS

This work was supported by a grant from Lawrence Livermore National Laboratory, purchase order No. 2846301. I would like to thank Donald Kingman and Konrad Yu for their help in setting up my experiments, and Robin McClure and Joyce Gianelli for typing the thesis.

REFERENCES

1. S. S. Ordan'yan, G. S. Tabatadze and L. V. Kozlovskii, Sov. Powder Met., Vol. 18, No. 7, p. 458 (1979).
2. A. G. Merzhanov, G. G. Karyuk, and I. P. Borovinskaya, Sov. Powder Met., Vol. 20, No. 10, p. 709 (1981).
3. A. G. Merzhanov and I. P. Borovinskaya, Acad. Sci. USSR Chem. Phys., Vol. 204, No. 2, pp. 366 (1972).
4. A. R. Sarkisyan, S. K. Dolukhanyan and I. P. Borovinskaya, Sov. Powder Met., Vol. 17, No. 6, p. 424 (1978).
5. O. R. Bergmann and J. Barrington, J. Amer. Cer. Soc., Vol. 49, No. 9, p. 502 (1966).
6. V. M. Shkiro, V. K. Prokudina, and I. P. Borovinskaya, Sov. Powder Met., Vol. 21, No. 12, p. 868 (1982).
7. L. B. Nezhevenko, V. I. Groshev, B. D. Gurevich, and O. V. Bokov, Refractory Carbides, G. V. Samsonov Ed., Consultants Bureau, New York, p. 89 (1974).
8. V. M. Shkiro, I. P. Borovinskaya, and A. G. Merzhanov, Sov. Powder Met., Vol. 18, No. 10, p. 684 (1979).
9. R. E. Nightingale, Fundamentals of Refractory Compounds, p. 203, H. H. Hausner and M. G. Bowman eds., Plenum Press, New York (1968).
10. E. K. Storms, The Refractory Carbides, Academic Press, New York (1967).
11. J. L. Chermant, H. Coster, and B. L. Mordike, Sci. Sintering, Vol. 12, No. 3, p. 171 (1980).

REFERENCES (continued)

12. I. P. Kushtalova, Sov. Powder Met., Vol. 6, No. 8, p. 606 (1967).
13. G. F. Samsonov and S. N. Bozhko, Sov. Powder Met., Vol. 8, No. 7, p. 542 (1969).
14. V. Ya. Naumenko, Sov. Powder Met., Vol. 8, No. 9, p. 764 (1969).
15. J. Vavrda and J. Blazikova, Sov. Powder Met., Vol. 18, No. 11, p. 850 (1979).
16. W. D. Kingery, K. K. Bowen, D. R. Uhlmann, Introduction to Ceramics, 2nd ed, p. 450, John Wiley and Sons, New York (1976).
17. P. Costa and R. R. Conte, Compounds of Interest in Nuclear Reactor Technology, I. Wuber and P. Chiotti eds., p. 784, The Metals Soc. AIME, Michigan (1964).
18. S. Sarian, J. App. Phys., Vol. 39, No. 7, p. 3305 (1968).
19. S. Sarian, J. App. Phys., Vol. 39, No. 11, p. 5036 (1968).
20. V. S. Bremeev and A. S. Panov, Sov. Powder Met., Vol. 6, No. 7, p. 65 (1967).
21. S. Sarian, J. App. Phys., Vol. 40, No. 9, p. 3515 (1969).
22. B. D. Cullity, Elements of X-Ray Diffraction, 2nd ed, p. 357, Addison-Wesley, Menlo Park, CA (1978).
23. D. L. Johnson and I. B. Cutler, J. Amer. Ceram. Soc., Vol. 46, No. 11, p. 541 (1963).

REFERENCES (continued)

24. S. S. Ordan'yan, A. E. Kravchik, and V. S. Neshpor, Sov. Powder Met., Vol. 16, No. 12, p. 952 (1977).
25. R. A. Andrievskii, v. V. Klimenko, V. I. Mitrofanov, and N. I. Poltoratskii, Sov. Powder Met., Vol. 16, No. 6, p. 423 (1977).
26. R. A. Andrievskii, I. I. Spivak, and K. L. Chevasheva, Sov. Powder Met., Vol. 7, No. 7, p. 559 (1968).
27. S. S. Ordan'yan, A. I. Augustinik, and L. V. Kudryasheva, Sov. Powder Met., Vol. 7, No. 8, p. 612 (1968).
28. P. S. Kislyi and M. A. Kuzenkova, Sov. Powder Met., Vol. 12, No. 2, p. 116 (1973).
29. A. E. Kravchik, G. A. Savel'ev, V. S. Neshpor, and S. S. Ordan'yan, Sov. Powder Met., Vol. 16, No. 3, p. 163 (1977).

Appendix: Data used in Figures 6 - 12

Kinetic Data Use for the Plots of Commercial (Starck) Powder.

Time Min.	Temp K	$\Delta V/V_0$	ρ_0 %	ρ %	$\Delta\rho/\rho_0$
60	1637	0.116	66.2	74.9	0.131
202	1639	0.184	65.5	80.3	0.225
1062	1635	0.266	66.0	89.9	0.362
122	1636	0.149	65.6	77.1	0.175
322	1639	0.209	65.1	82.3	0.264
420	1663	0.288	65.2	91.6	0.404
120	1665	0.184	65.5	80.2	0.225
56	1667	0.143	65.8	76.8	0.167
195	1666	0.233	65.7	85.6	0.304
1015	1666	0.310	65.3	94.6	0.449
214	1471	0.058	65.4	69.4	0.061
120	1471	0.050	65.5	68.9	0.053
400	1470	0.065	65.9	70.5	0.069
60	1475	0.036	65.6	68.0	0.037
927	1470	0.097	65.2	72.2	0.107
208	1539	0.096	66.0	73.0	0.106
1024	1538	0.204	65.6	82.4	0.256
120	1541	0.073	65.7	70.9	0.079
400	1538	0.123	65.5	74.7	0.140
60	1537	0.056	65.6	69.5	0.059

Kinetic Data, Commercial (Starck).

Time Min.	Temp K	DV/V_0	ρ_0 %	ρ %	$\Delta\rho/\rho_0$
928	1552	0.204	65.7	82.5	0.256
277	1553	0.129	65.4	75.0	0.147
204	1555	0.110	65.6	81.3	0.124
60	1554	0.065	66.0	70.6	0.069
120	1553	0.089	65.2	71.5	0.096
1016	1490	0.116	65.1	73.6	0.131
195	1492	0.061	65.2	69.4	0.065
360	1491	0.077	65.9	71.4	0.083
60	1494	0.034	65.3	67.5	0.034
120	1493	0.046	65.7	68.8	0.048

Arrhenius Data for Commercial (Starch) Powder.

Temp K	$\Delta V/V_0$	ρ_0 %	ρ %	$\Delta \rho/\rho_0$
1533	0.059	65.8	69.8	0.061
1433	0.024	65.7	67.2	0.023
1633	0.106	66.0	73.6	0.115
1637	0.116	66.2	74.9	0.131
1433	0.030	66.1	68.1	0.030
1593	0.076	65.5	70.8	0.081
1475	0.036	65.6	68.2	0.039
1537	0.056	65.6	69.4	0.058
1494	0.034	65.3	67.5	0.034
1617	0.099	64.7	72.1	0.110
1667	0.143	65.8	76.5	0.163
1733	0.186	65.1	79.5	0.222
1695	0.183	65.4	79.4	0.214
1554	0.065	66.0	70.6	0.069

Arrhenius Data for SYN 1 Powder.

Temp K	$\Delta V/V_0$	ρ_0 %	ρ %	$\Delta \rho/\rho_0$
1726	0.097	66.0	73.0	0.107
1667	0.064	64.9	69.3	0.068
1637	0.057	65.5	69.4	0.060
1538	0.026	65.9	67.6	0.027
1587	0.036	65.6	68.0	0.037
1615	0.031	65.3	67.4	0.032
1695	0.091	65.3	72.4	0.100
1753	0.100	66.0	73.3	0.111
1786	0.134	65.6	75.7	0.155
1470	0.023	65.4	66.9	0.023

Kinetic Data for SYN 1 Powder.

Time Min.	Temp K	$\Delta V/V_0$	ρ_0 %	ρ %	$\Delta \rho/\rho_0$
60	1726	0.097	66.0	73.0	0.107
120	1725	0.109	65.7	73.7	0.122
425	1722	0.192	65.5	81.0	0.237
1010	1724	0.265	65.3	88.8	0.360
194	1723	0.138	65.4	75.8	0.160
420	1663	0.131	65.3	75.2	0.151
120	1665	0.083	65.7	71.6	0.090
56	1667	0.064	64.9	69.3	0.068
195	1666	0.092	66.1	72.8	0.101
1015	1666	0.190	65.5	80.8	0.234
60	1637	0.057	65.5	69.4	0.060
202	1639	0.081	65.3	71.0	0.088
1062	1635	0.152	66.1	77.9	0.179
122	1636	0.074	65.4	70.6	0.080
322	1639	0.092	66.2	72.9	0.101
20	1539	0.030	65.4	67.4	0.031
400	1538	0.036	66.1	68.6	0.037
1024	1538	0.042	65.1	67.9	0.044
60	1538	0.026	65.9	67.6	0.027
120	1541	0.028	65.7	67.6	0.029

Kinetic Data for SYN 5 Powder.

Time Min.	Temp K	$\Delta V/V_0$	$\bar{\rho}_0$ %	ρ %	$\Delta \rho/\rho_0$
205	1724	0.118	67.8	76.9	0.134
60	1724	0.079	68.8	74.7	0.086
120	1725	0.099	67.9	75.4	0.110
1753	220	0.148	68.0	78.8	0.174
1754	60	0.089	68.3	75.0	0.097
1753	120	0.117	67.7	76.0	0.132
1849	60	0.145	68.1	80.0	0.175
1850	120	0.190	67.9	83.8	0.234
1850	215	0.241	68.0	89.6	0.317
1790	60	0.108	67.8	76.0	0.121
1788	130	0.143	68.4	79.8	0.167
1791	245	0.195	68.2	84.7	0.242

Kinetic Data for SYN 7 Powder.

Temp. K	Time Min.	$\Delta V/V_0$	ρ_0	ρ	$\Delta\rho/\rho_0$
1613	60	0.175	66.0	80.0	0.212
1614	334	0.224	67.3	86.7	0.289
1612	130	0.195	67.0	83.2	0.242
1500	272	0.126	68.2	78.0	0.144
1501	60	0.096	67.4	74.5	0.106
1500	130	0.109	67.1	75.3	0.122
1562	260	0.174	67.5	81.7	0.210
1562	60	0.135	67.2	77.7	0.156
1563	120	0.151	67.0	78.9	0.178
1448	60	0.074	67.3	72.8	0.080
1448	120	0.084	66.9	73.0	0.092
1449	220	0.095	67.6	74.7	0.105

Arrhenius Data for SYN 7 Powder

Temp. K	$\Delta V/V_0$	ρ_o %	ρ %	$\Delta \rho/\rho_o$
1406	0.066	67.2	72.0	0.071
1448	0.074	67.4	72.8	0.080
1510	0.105	67.6	75.5	0.117
1613	0.175	66.0	80.0	0.212
1562	0.135	67.2	77.7	0.156
1500	0.096	67.4	74.5	0.106

Arrhenius Data for SYN 5 Powder.

Temp. K	$\Delta V/V_0$	ρ_o %	ρ %	$\Delta \rho/\rho_o$
1698	0.067	68.0	72.9	0.072
1848	0.148	67.7	79.5	0.174
1649	0.063	68.1	72.6	0.067
1763	0.091	68.0	74.8	0.100
1785	0.106	68.2	75.1	0.118
1754	0.089	68.3	75.0	0.097
1724	0.079	68.8	74.7	0.086